Solid State Ionics 57 (1992) 345–351
North-Holland

SOLID STATE IONICS

Raman scattering and ionic transport in $SrCe_{1-x}Yb_xO_3$

I. Kosacki [1], J. Schoonman
Laboratory for Inorganic Chemistry, Delft University of Technology, Julianalaan 136, 2628 BL Delft, The Netherlands

and

M. Balkanski
Laboratorie de Physique des Solides associe au CNRS, Université Pierre et Marie Curie, 4 Place Jussieu, 75252 Paris Cedex 05, France

Received 10 April 1992; accepted for publication 21 April 1992

The results of Raman scattering and ionic conductivity measurements for $SrCe_{1-x}Yb_xO_3$ are presented. The observed Raman spectrum was interpreted on the basis of factor-group analysis for the group D_{2h}^{16}. The effect of the influence of ytterbium ions on the dynamical and electrical properties of $SrCe_{1-x}Yb_xO_3$ is discussed. A correlation between ionic transport and vibrational properties will be presented.

1. Introduction

The perovskite oxides based on $SrCeO_3$ exhibit at high temperatures proton conduction in hydrogen containing atmospheres [1,2]. $SrCeO_3$ doped with trivalent cations: Yb, Y, Sc, belongs to this type of proton conductors and was first reported by Iwahara et al. [2,3]. These materials can be used in many solid state electrochemical devices such as fuel cells, steam electrolyzers and gas sensors [4,5].

However, the proton migration mechanism has not been determined in detail. Two models have been proposed to describe the dynamics of the proton transport.

The first is the "free migration" mechanism: the proton moves by jumping between stationary host oxygen ions. In the other process, the "vehicle mechanism", the proton moves as a passenger on a larger ion, such as OH^- or H_3O^+ [6]. This latter conductivity mechanism can be confirmed by IR-absorption measurements, in which it is possible to monitor OH^- stretching vibrations [5,7].

[1] Permanent address: Technical University of Radom, ul. Malczewskiego 29, 26-600 Radom, Poland.

Our recent electrical conductivity measurements of $SrCe_{0.95}Yb_{0.05}O_3$ in atmospheres with different hydrogen concentrations [8] show that the surrounding hydrogen atmosphere has no effect on the bulk conductivity. This fact indicates that the conduction mechanism is more complex than a simple free migration process or a vehicle mechanism.

Probably the dopant Yb ions in $SrCeO_3$ play an essential role in the proton transport. Since pure $SrCeO_3$ exhibits only low electronic conductivity, oxygen ion vacancies or electron holes, which are generated by partial substitution of Ce^{4+} by aliovalent cations such as Yb^{3+}, seem to play an important role in the proton conduction mechanism in this material.

In order to understand the relationship between the conductivity, the structure and the composition of $SrCe_{1-x}Yb_xO_3$ one needs to understand in some detail the dynamical behavior of the ionic species.

Ionic transport and the vibrational properties of crystals are determined by the interactions between the crystal lattice ions. This interaction, as shown for $Cd_{1-x}Pb_xF_2$ crystals, can be determined from infrared and Raman measurements [9]. These meth-

0167-2738/92/$ 05.00 © 1992 Elsevier Science Publishers B.V. All rights reserved.

ods are important for the study of ion disordering in fast ion conductors.

The use of vibrational spectroscopy to study the lattice dynamics of perovskite-type crystals has been carried out by several authors [10–13]. These investigations were focused on the relation between ferroelectricity and lattice dynamics [13]. Vibrational spectroscopy is a powerful and sensitive experimental technique to study dynamical processes. It can be important in advancing the understanding of the proton conductivity mechanism in the present material. For this reason, the authors have conducted a Raman spectroscopic study of $SrCe_{1-x}Yb_xO_3$. The Raman spectra of this material have not been studied previously.

In this paper, the results of Raman scattering and ionic conductivity measurements for $SrCe_{1-x}Yb_xO_3$ are presented. The aim of this work is to study the influence of Yb^{3+} ions and H_2-annealing on the vibrational and electrical properties of $SrCe_{1-x}Yb_xO_3$, and to find a correlation between the concentration of Yb^{3+} ions and oxygen ion vacancies, which are formed during the substitution of Ce^{4+} by Yb^{3+} in this material.

2. Samples and experimental details

$SrCe_{1-x}Yb_xO_3$ ceramic samples were obtained using the procedure of Iwahara [4]. A well determined mixture of $SrCO_3$ (99.4% supplied by Johnson Mattey) CeO_2 (99.999% Janssen Chemica) and Yb_2O_3 (99.9% Fluka Chemie) was carefully prepared and calcined at 1673 K for 10 h in air. The calcined oxides were subsequently milled, shaped into pellets via cold isostatic pressing and finally sintered at 1823 K for 10 h.

The $SrCe_{1-x}Yb_xO_3$ samples obtained in this way were then investigated using Raman spectroscopy. The Raman spectra were recorded at room temperature in the frequency range (30–1000)cm^{-1} using a Jobin–Yvon "U1000" double monochromator equipped with two holographic gratings. The light scattering was detected with an ITT FW130 cooled photo multiplier coupled with a computerized photon-counting system. The excitation source was the 5145 Å line of an Ar^+ ion laser at a power level of 40 mW.

The observed Raman spectra were interpreted on the basis of space-group analysis for the Pnma-D_{2h}^{16} group symmetry. The ionic conductivity was determined from impedance measurements which were performed using a Solartron 1260 Frequency Response Analyzer. The spectra were recorded in the frequency range of 0.1 Hz to 10 MHz at temperatures in the region from 450 to 1100 K in air.

3. Group-theoretical analysis

The structure of $SeCeO_3$ and $SrCe_{0.95}Yb_{0.05}O_3$ has been studied by X-ray diffraction techniques. The structure of these materials is orthorhombic with a tilted octahedron system with four formula units in the primitive cell. Fig. 1 presents the structure of $SrCeO_3$ with ion distances which were determined by the Rietveld method [14]. The factor group of orthorhombic perovskite $SrCeO_3$ was assumed to be Pnma-D_{2h}^{16}, similar to the space group determined by Kay and Bailey [11,13] for $CaTiO_3$.

There are 20 atoms in the unit cell implying a total 57 (3n-3) optical vibrational modes. The site symmetry of all atoms is available from X-ray scattering data [14]. This allows us to make a detailed group-theoretical analysis of the long-wavelength zone center optical phonons [15]. Factor group analysis for

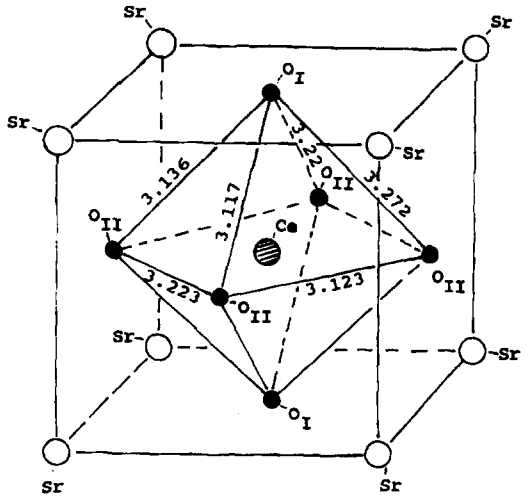

Fig. 1. Crystal structure of the perovskite $SrCeO_3$. The ion distances are in Å [14].

Table 1
The Raman mode symmetry in $SrCeO_3$ as determined from group-theoretical analysis.

Atom	Raman mode symmetry
Sr(4c)	$2A_g+B_{1g}+2B_{2g}+B_{3g}$
O_I(4c)	$2A_g+2B_{2g}+B_{1g}+B_{3g}$
O_{II}(8d)	$3A_g+3B_{2g}+3B_{1g}+3B_{3g}$
Ce(4a)	not Raman active

the $SrCeO_3$ orthorhombic structure gives the following optical modes:

$$7A_g(R)+5B_{1g}(R)+7B_{2g}(R)+5B_{3g}(R)+8A_u$$
$$+9B_{1u}(IR)+7B_{2u}(IR)+9B_{3u}(IR)\,.$$

Infrared-active phonons (IR) have B_{iu} symmetries, while the Raman-active phonons (R) have A_g and B_{ig} symmetries.

The site symmetry of all atoms [14] and Raman mode symmetry in $SrCeO_3$ determined from group-theoretical analysis are given in table 1. The Wyskoff site notation has been used to describe the mode symmetries [15]. The vibrations related with oxygen ions (18) and strontium ions (8) add up to a total of 24 Raman active modes. Among fully symmetric A_g vibrations 2 modes are due to Sr ion contribution, 2 modes to O_I ion contribution and 3 modes to O_{II} ion contribution. Sr, O_I, O_{II} ions contribute also to B_{1g}, B_{2g} and B_{3g} vibrations. The Ce^{4+} ions have C_i site symmetry and vibrations involving these ions are not active in Raman scattering.

The introduction of Yb ions into $SrCeO_3$ will not change the crystal symmetry [14]. Therefore our discussion of Raman modes symmetry for $SrCeO_3$ can be also applied for $SrCe_{1-x}Yb_xO_3$. Consequently, the introduction of Yb will not change dramatically the Raman spectrum because the introduction of Yb ions into $SrCeO_3$ can only influence Raman lines which are connected with oxygen ion contributions to Raman modes. Any influence on Raman lines connected with strontium is considered to be unlikely.

4. Experimental results and discussion

Fig. 2 presents the Raman spectra of $SrCe_{1-x}Yb_xO_3$. Based on the above presented group-theoretical analysis results the Raman vibrations in $SrCe_{1-x}Yb_xO_3$ were analyzed.

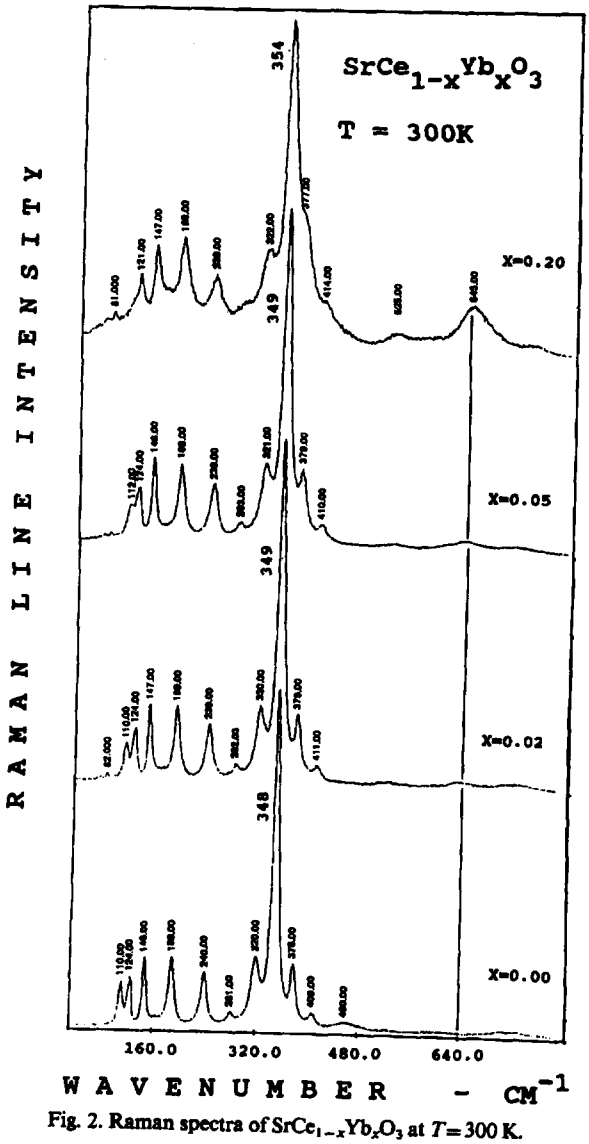

Fig. 2. Raman spectra of $SrCe_{1-x}Yb_xO_3$ at $T=300$ K.

The lines at frequencies 110, 124, 146, 240, and 281 cm^{-1} are probably vibrations involving strontium ions. This hypothesis is confirmed by the independence of intensity and frequency behavior with Yb^{3+} concentration.

Since Yb^{3+} and Ce^{4+} ions are screened by oxygen ions, the influence of the substitution of Ce^{4+} by Yb^{3+} ions on vibrations involving strontium can be neglected in first approximation.

The Raman lines at 320, 348 and 378 cm^{-1} are probably connected with vibrations involving oxygen ions. These vibrations constitute a vibration of O_{II} ions around the oxygen octahedron axis. Since the oxygen octahedron has three unique C_3 axes these vibrations are triply degenerate in the perovskite structure [12]. Only one of them is stabilized by vibrations about a single axis. The other two possible vibrations are assumed to have only secondary effects.

In the case of $SrCe_{1-x}Yb_xO_3$ (fig. 2) this effect is manifested in a low intensity of the lines at 320 and 378 cm^{-1} with respect to the 348 cm^{-1} line. The 348 cm^{-1} Raman line is connected with vibration of AO_6 octahedra (A=Yb or Ce). The frequency and shape is changed with Yb concentration. The effect of substitution of Ce^{4+} by Yb^{3+} ions in $SrCe_{1-x}Yb_xO_3$ is manifested in the Raman spectra of these materials (fig. 2). The influence of Yb doping is observed in broadening of the 348 cm^{-1} Raman line. This broadening is probably induced by local distortions around the Yb^{3+} ions. There exists a correlation between the half-width of the 348 cm^{-1} line and the Yb concentration as is shown in fig. 3.

The introduction of Yb ions into the $SrCeO_3$ lattice generates oxygen ion vacancies. When Yb^{3+} replaces Ce^{4+} negative point defects are generated. These defects are believed to be compensated by oxygen ion vacancies with one vacancy for every two Yb^{3+} ions. The presence of oxygen ion vacancies in $SrCe_{1-x}Yb_xO_3$ is confirmed by the Raman scattering measurements. An additional line at 640 cm^{-1} which is not present in the spectrum of pure $SrCeO_3$ has been observed (fig. 2). The intensity of this line is a linear function of the Yb concentration (fig. 4). This line is probably connected with an oxygen ion vacancy of which the concentration is determined by the Yb concentration.

The introduction of Yb^{3+} ions into $SrCeO_3$ will be accompanied with the introduction of oxygen ion vacancies, which shall change the local symmetry and hence induce the Yb–O symmetric stretching vibration at frequency 640 cm^{-1}. In orthorhombic symmetry this vibration is not Raman active (table 1). Similar lines were observed for $CaTiO_3$ at 639 cm^{-1} [11] and for $CaHfO_3$ at 590 cm^{-1} [16]. These bands

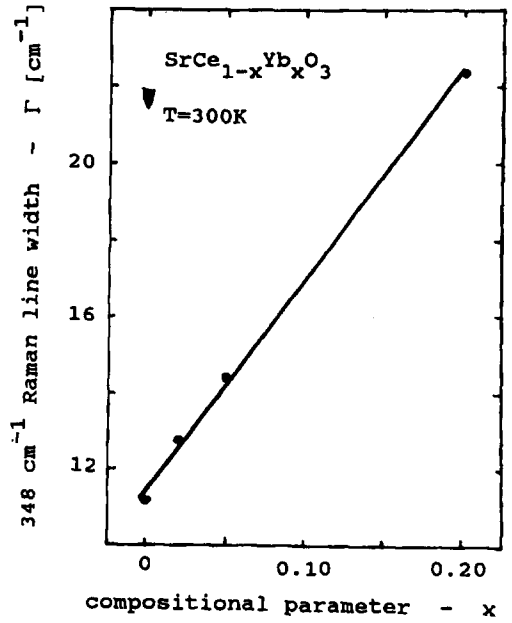

Fig. 3. The compositional dependence of the half-width of the 348 cm^{-1} Raman line for $SrCe_{1-x}Yb_xO_3$.

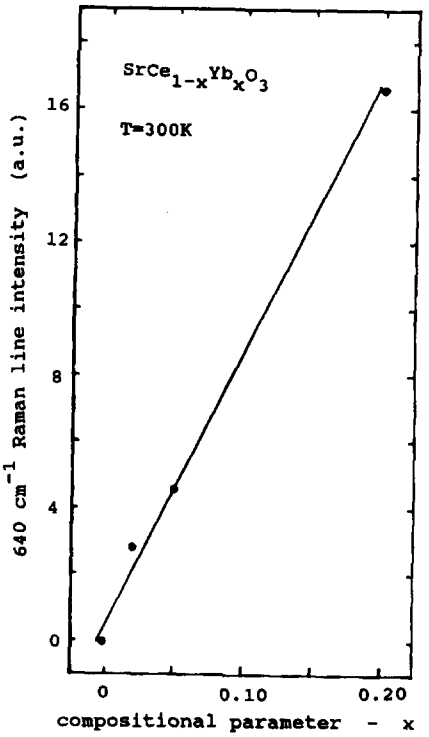

Fig. 4. The compositional dependence of the intensity of the 640 cm^{-1} Raman line for $SrCe_{1-x}Yb_xO_3$.

are related to Ti–O and Hf–O symmetric stretching vibrations.

Additional confirmation of the present hypothesis is found in the results of annealing $SrCe_{1-x}Yb_xO_3$ in a reducing hydrogen atmosphere. Fig. 5 presents the Raman spectrum of $SrCe_{0.95}Yb_{0.05}O_3$ after annealing in H_2 at a temperature of 500°C during four hours. The result of this annealing procedure is similar to Yb doping. A broadening of the line at 348 cm^{-1} is observed from a line width $\Gamma = 14.4$ cm^{-1} to $\Gamma = 21$ cm^{-1} both after annealing and after doping. An increase of the 640 cm^{-1} line intensity is observed too. The measure for it may be the ratio of the intensity of this line and the intensity of the line at 348 cm^{-1} i.e. I_{640}/I_{348}. For $SrCe_{0.95}Yb_{0.05}O_3$ before annealing in hydrogen this ratio equals 0.043. After annealing the ratio attains a higher value and equals 0.210 and is similar to the value for not annealed $SrCe_{0.8}Yb_{0.2}O_3$, which equals 0.166.

The results presented above confirm the relation of the Raman line at 640 cm^{-1} in $SrCe_{1-x}Yb_xO_3$ and the defect structure. The introduction of ytterbium ions into $SrCeO_3$ induces oxygen ion vacancies which are compensating the substitution of Ce^{4+} ions by Yb^{3+}. These vacancies induce the new Raman band at a frequency of 640 cm^{-1} which is connected with an Yb–O symmetric stretching vibration.

The presence of oxygen ion vacancies must influence the electrical properties of $SrCe_{1-x}Yb_xO_3$. The introduction of Yb^{3+} ions is manifested by a rise in the ionic conductivity and a drop in the activation energy, as shown in fig. 6. For pure $SrCeO_3$, the conductivity activation energy has a value of 1.02 eV.

In the case of $SrCe_{1-x}Yb_xO_3$, the activation energy is rapidly decreasing between $0<x<0.02$ and is practically constant for the concentration $0.02<x<0.2$. The conductivity activation energy for $SrCe_{1-x}Yb_xO_3$, determined from the Arrhenius plots (fig. 6) attains values of 0.67 eV, 0.65 eV and 0.63 eV for $x=0.02$, 0.20 and 0.05, respectively. These values are in very good accordance with reported re-

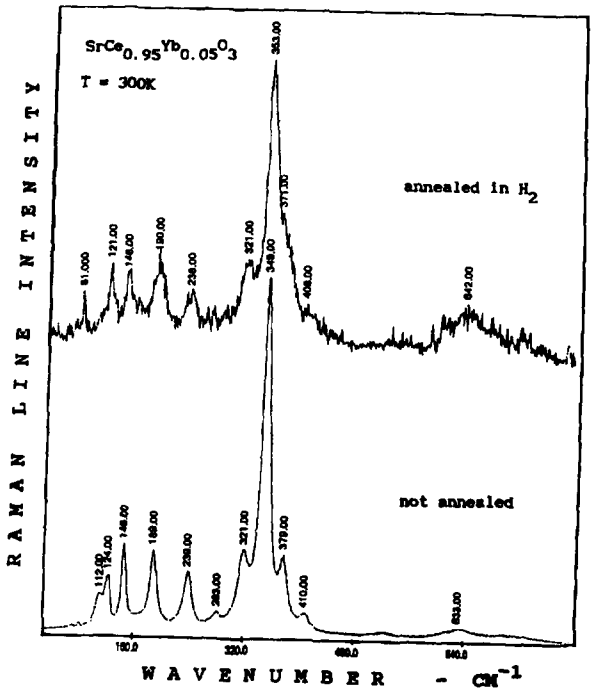

Fig. 5. Raman spectrum of $SrCe_{0.95}Yb_{0.05}O_3$ annealed in hydrogen atmosphere.

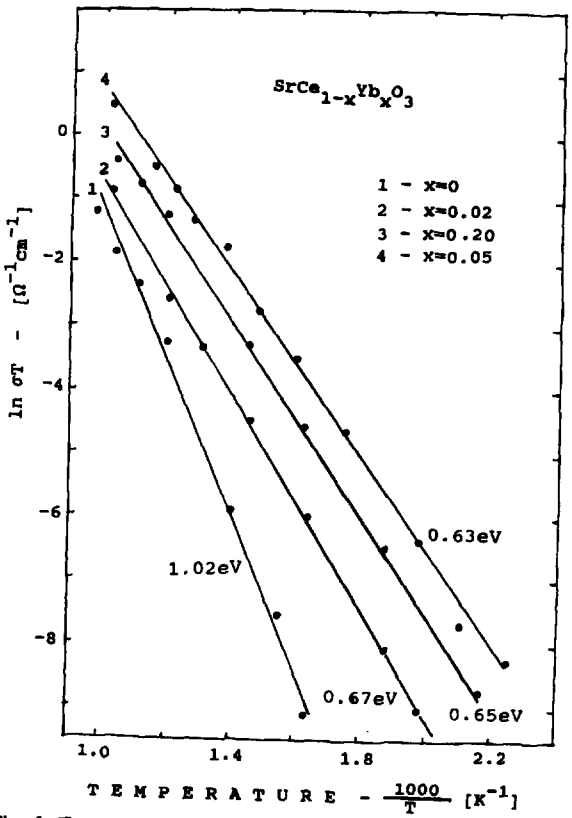

Fig. 6. Temperature dependence of the ionic conductivity for $SrCe_{1-x}Yb_xO_3$. Compositions and the activation energy of conductivity are in the figure.

sults of 0.63 eV [3] and 0.67 eV [3,17].

It should be mentioned that these latter values were determined for $SrCe_{0.95}Yb_{0.05}O_3$ in hydrogen or air atmospheres.

The above presented variations of the conductivity activation energy with the ytterbium indicate that the predominant mechanism of ionic conductivity in $SrCeO_3$ is the migration of oxygen ions. This hypothesis is confirmed by the rapid decrease of the conductivity activation energy with increasing Yb ion concentration.

While the introduction of Yb^{3+} ions increases the ionic conductivity, the compositional dependence is not monotonic and attains a maximum for $x=0.05$ (fig. 6). This is probably connected with a change in carrier mobility, which drops down when a certain level of Yb concentration in $SrCe_{1-x}Yb_xO_3$ is exceeded.

Additional information about the transport mechanism in $SrCe_{1-x}Yb_xO_3$ can be obtained from dielectric relaxation measurements. This technique is complementary to electrical conductivity and provides information relating to the local motion of bound defect pairs constituting an electric dipole. For example dielectric relaxation was used to study the substitution of Ba by La ions in $Ba_{1-x}La_xF_{2+x}$ fluorite crystals [18]. The electrical properties of these concentrated solid solutions are dominated by the formation of defects clusters, formed by aggregation of two or more substitutional cations and a number of charge compensating anion defects. We have conducted dielectric relaxation measurements of $SrCe_{0.95}Yb_{0.05}O_3$, which is characterized by the highest conductivity (fig. 6).

Fig. 7 presents the dependence of the dielectric loss function – $\tan\delta$ on the angular frequency for $SrCe_{0.95}Yb_{0.05}O_3$ measured at different temperatures. For temperatures below 300°C, two dielectric relaxation peaks are observed. At higher temperatures only one relaxation peak is present. With increasing temperature the maxima shift towards higher frequencies. From the temperature dependence of the frequency at which the loss function attains a maximum, ω_{max}, the activation energy of the relaxation phenomena has been determined by using the Arrhenius equation $\ln(\omega_{max}^{-1})=\ln\tau_0+E(kT)^{-1}$. The lower frequency peak was used for this calculation. For $SrCe_{0.95}Yb_{0.05}O_3$ the activation energy attains a value of 0.70 eV, which is similar to the conductivity activation energy obtained from the impedance spectra (fig. 6).

This result strongly suggests that the dipolar relaxation is due to a complex defect in which the oxygen ion vacancy can exhibit localized motion. The

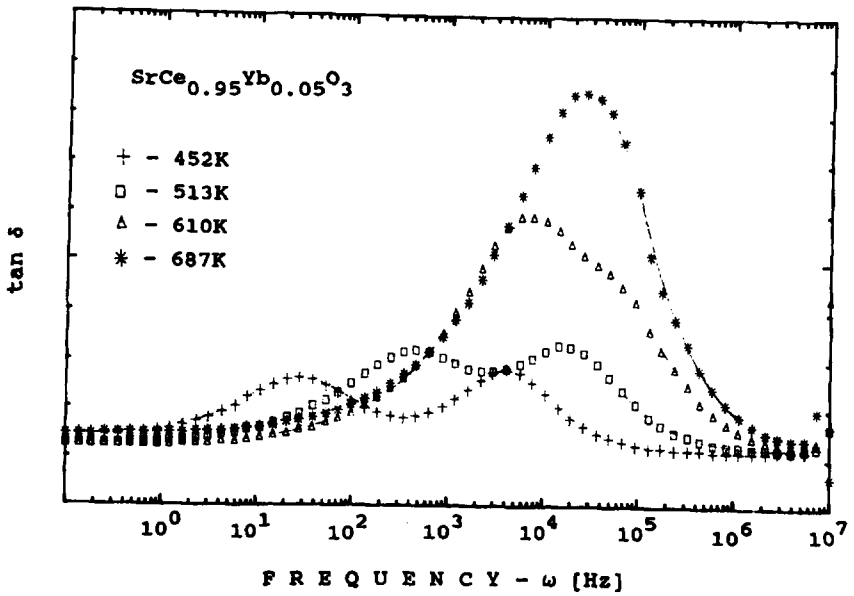

Fig. 7. Variation of the loss function, tan δ, with frequency for $SrCe_{0.95}Yb_{0.05}O_3$ at different temperatures.

most simple defect complex is the associate $(Yb_{Ce}\cdot V_O)^{\cdot}$; in which the dopant ion is immobile. The reorientation of the vacancy proceeds via a similar mechanism as the conduction mechanism. For large concentration of dopant ions a percolation-type of ionic conductivity can occur, in which the vacancies hop from one dopant ion to the other without changing the number of dipoles. Both dielectric relaxation peaks observed in the $SrCe_{0.95}Yb_{0.05}O_3$ samples may be due to dipoles involving to Yb dopant, as is evidenced by the absence of such peaks in undoped $SrCeO_3$.

Similar results have been obtained for dielectric relaxation measurements of $KTaO_3$ doped with Fe [19]. This author has observed also two relaxation peaks which were interpreted to be due to $(Fe_{Ta}\cdot V_O)^{\times}$ and possibly $(Fe_{Ta}\cdot V_O)^{\cdot}$ defect pairs [19]. However, in our case the second peak may also be related to grain boundary polarization phenomena. This is presently under study.

4. Conclusions

On the basis of the presented results of the $SrCe_{1-x}Yb_xO_3$ Raman scattering it is concluded that the substitution of Ce^{4+} ions by Yb^{3+} changes the shape of the 348 cm^{-1} line. This vibration involves the oxygen octahedron (A_g symmetry). A linear dependence between the ytterbium concentration and the 348 cm^{-1} Raman line half-width has been found.

Introduction of Yb ions induces the formation of oxygen ion vacancies. The presence of oxygen ion vacancies in $SrCe_{1-x}Yb_xO_3$ is confirmed by the Raman scattering measurements. In this material an additional line at 640 cm^{-1} is observed with an intensity linearly dependent on the Yb concentration. This line may be connected with Yb–O stretching vibrations, which become Raman-active because of the loss of local symmetry by the presence of oxygen ion vacancies in $SrCe_{1-x}Yb_xO_3$. These vacancies may occupy positions between two Yb^{3+} ions and are compensating the substitution of Ce^{4+} by Yb^{3+} ions. The oxygen ion vacancies play an essential role in the ionic conductivity mechanism in this material.

The introduction of Yb ions into $SrCeO_3$ is manifested by a rise in the ionic conductivity and drop in the conductivity activation energy. The dielectric relaxation measurements, indicate that the ionic conductivity in $SrCe_{1-x}Yb_xO_3$ is connected with reorientation of oxygen ion vacancies with respect to Yb ions in a percolation-type of mechanism.

Acknowledgement

One of the authors (I.K.) wishes to thank Dr. A.P. Litvinchuk for his help in the group-theoretical analysis of $SrCeO_3$ and Dr. Ir. J.G.M. Becht for constructive discussions.

References

[1] H. Uchida, H. Yoshikawa and H. Iwahara, Solid State Ionics 34 (1989) 103.
[2] H. Iwahara, T. Esaka, H. Uchida and N. Maeda, Solid State Ionics 3/4 (1981) 359.
[3] T. Scherban and A.S. Nowick, Solid State Ionics 35 (1989) 189.
[4] H. Iwahara, H. Uchida, K. Ogaki and H. Nagato, J. Electrochem. Soc. 138 (1991) 295.
[5] H. Uchida, H. Kimura and H. Iwahara, J. Appl. Electrochem. 20 (1990) 390.
[6] T. Norby, Solid State Ionics 40/41 (1990) 857.
[7] S. Shin, H.H. Huang, M. Ishigame and H. Iwahara, Solid State Ionics 40/41 (1990) 910.
[8] F. De Schutter, J. Vangrunderbeek, J. Luyten, I. Kosacki, R. Van Landschoot, J. Schram and J. Schoonman, Solid State Ionics 57 (1992) 77.
[9] I. Kosacki, Appl. Phys. A 49 (1989) 413.
[10] A.E. Pasto and R.A. Condrate, J. Am. Ceram. Soc. 56 (1973) 436.
[11] U. Balachandran and N.G. Eror, Solid State Commun. 44 (1982) 815.
[12] L.L. Boyer and J.R. Hardy, Phys. Rev. B 24 (1981) 2577.
[13] P.F. Mc Millan and A.M. Hofmeister, in: Reviews in Mineralogy, ed. F.C. Hawthorne, Vol. 18, Spectroscopic Methods in Mineralogy and Geology (Mineralog. Soc. of America, Chelsea, MI, 1988) p. 99.
[14] A. Saki, Y. Seto, N. Ishizawa, M. Kato and N. Mizutanu, Nippon Kagaku Kaishi 1 (1991) 25.
[15] D.L. Rousseau, R.P. Bauman and S.P.S. Porto, J. Raman Spectrosc. 10 (1973) 253.
[16] C.I.L. Park, R.A. Condrate and R.L. Snyder, Appl. Spectrosc. 30 (1976) 352.
[17] N. Bonanos, B. Ellis and M.N. Mahmood, Solid State Ionics 28/30 (1988) 597.
[18] A. Roos, D.R. Franceschetti and J. Schoonman, J. Phys. Chem. Solids 46 (1985) 645.
[19] T. Scherban, Ph.D. Thesis (Columbia University, NY, 1991); and private communication.